Enhancing the Welding-Technological Properties of Electrodes through a Nanostructured Activating Component

Rustam Saidov
Laboratory of Nanostructured Materials and Devices on Them, Institute of Material Sciences, Academy of Science of Uzbekistan, Tashkent, Uzbekistan
saidov_r@yahoo.com

Rustam Rakhimov
Laboratory of Nanostructured Materials and Devices on Them, Institute of Material Sciences, Academy of Science of Uzbekistan, Tashkent, Uzbekistan
rustam-shsul@yandex.com

Kamel Touileb
Department of Mechanical Engineering, College of Engineering in Al-Kharj, Prince Sattam bin Abdulaziz University, Al-Kharj, Saudi Arabia
K.touileb@psau.edu.sa (corresponding author)

Sun L.Y.
Institute of New Materials, Guangdong Academy of Sciences, Guangzhou, China
sunliying_48@163.com

B. D. Yusupov
Department of Technologic Machines and Equipment, Almalyk State Technical Institute, Almalyk, Uzbekistan
yusupov.b.d@gmail.com

Received: 21 December 2025 | Revised: 18 January 2026 and 4 February 2026 | Accepted: 7 February 2026

 DOI: https://doi.org/10.48084/etasr.17095

ABSTRACT

This study aims to investigate the effect of the special activating component A-815 on the welding and technological properties of a welding electrode when incorporated into the coating of a rutile welding electrode. This study introduces a novel synthesis method for Nanostructured Functional Ceramic (NFC) (A-815) using pulsed radiation activation. The coating additive significantly enhanced arc stability and deposition efficiency while reducing metal spatter and waste. The results showed the beneficial effect of doping the electrode with A-815 on the welding technological properties. The breaking length of the electrode arc increased by up to 10%, reducing the height of the visor at the end of the electrode by more than 33% and the coefficient of loss due to burnout and spattering by up to 12%. At the same time, the melting and surfacing coefficients were improved, since they increased by 17% when up to 16% of the activator was added. The molten metal losses of the electrode due to spattering and evaporation were significantly reduced.

Keywords-shielded metal arc welding; welding electrodes; electrode coating; activating component; nanostructured functional ceramics

I. INTRODUCTION

Flux is a mixture of minerals, silicates, carbonates, fluorides, and deoxidizers that protects the weld pool from atmospheric contamination. It can be found in various forms, including powder, paste, or as a coating on electrodes. Apart from welding, flux is used in the iron-making process. The Blast Furnace (BF) remains the primary technology in the

production of pig iron, accounting for over 90% of the latter [1]. The metallurgical properties of BF slags are highly determined by their viscosity. The ideal slag should have an appropriate viscosity that allows it to flow smoothly and remove most of the gangue minerals, facilitating efficient metal-slag separation. Activator oxides (fluxes), such as Al_2O_3-CaO-SiO_2 and SiO_2-Al_2O_3-MgO, are added to control slag viscosity. The viscosity impacts of the minor elements, including FeO, TiO_2, Na_2O, and K_2O was also considered in [2]. However, the surface tension of molten slag is a main factor in ironmaking and steelmaking processes for monitoring the surface and interfacial phenomena [3]. Activator oxide TiO_2 acts as a surfactant in the CaO–SiO_2–MgO–Al_2O_3–TiO_2 system, contributing to the decrease in the surface tension of the melt. The surface tension of the slag rises from 413 mN/m to 456 mN/m as the CaO/SiO_2 mass ratio increases from 0.90 to 1.20 [4].

Mold fluxes are also designed to have the capacity to absorb or entrap inclusions in the liquid slag–metal interface. Coarse particles can easily cross the slag/metal interface, but smaller inclusions require more time to do so. The absorption of inclusions can be enhanced using fluxes with high CaO/SiO_2 ratios [5]. Soldering flux is a crucial chemical agent used in soldering to facilitate the joining of metal surfaces, serving multiple purposes: it cleans the metal surfaces; prevents oxidation during heating, which can hinder bonding, ensuring that metal surfaces are clean for a strong bond; and promotes better wetting of the solder, confirming that it fills gaps and creates a strong, uniform bond. Welding flux is a significant material in the welding process that ensures weld integrity. The flux comprises complex chemical compounds that improve the weld quality and shield the weld pool from contaminants. Fluxes chemically react with these impurities, breaking them down into a slag that floats to the surface of the molten metal.

Many types of fluxes are commonly used in welding processes, such as Submerged Arc Welding (SAW) and Electro-Slag Welding (ESW), producing a slag that helps remove impurities from the weld. They are also employed in Gas Tungsten Arc Welding (GTAW), Gas Metal Arc Welding (GMAW), and laser welding, to improve the weld depth penetration. The flux in paste or spray form is applied to the surface of the metal being welded. The main function of a flux in welding is to protect the welding area from deleterious gases in the atmosphere and to enhance the depth of weld penetration, ensuring high productivity [6-10]. Authors in [11] stated that for TIG welding, with the presence of surfactant elements, the molten metal moves from the edges to the center of the weld pool; so, the weld bead is narrow and deep. Authors in [12, 13] considered that the vaporized element from the flux contributes to increasing the temperature at the anode because of the increase in current density and the higher arc voltage. Shielded Metal Arc Welding (SMAW) is a manual welding process that uses a consumable metal electrode, coated with a flux material. An arc is produced between a coated filler metal electrode and the workpiece to be welded [14-16]. SMAW is versatile and can be used in a wide range of industrial applications, including construction, oil and gas, maintenance and repair, shipbuilding, fabrication, automotive, and aerospace industries. SMAW can be learned easily due to its simplicity and ability to operate in various climatic conditions, both indoors and outdoors [17].

In [18], the ceramic material ZB-2, synthesized by deploying the pulsed radiation activation technology, demonstrated its efficiency when used as an additive in the coating charge of the MP-3 welding electrode. The results obtained showed an increase in the breaking length of the MP-3 welding electrode arc and its favorable effect on the quality of weld formation when up to 2% of ZB-2 was added to the coating charge. A decrease in the visor size at the end of the electrode was observed with the addition of ZB-2 to 1%. Increasing the content of this additive in the MP-3 electrode coating to 8% reduced the melting coefficient and increased the deposition coefficient, contributing to a sharp decrease in losses due to burnout and spatter to 53%.

The objective of this work is to conduct a comprehensive investigation into the effect of adding the activating component A-815 (ranging from 0 to 16 wt.%) on the welding-technological properties of the rutile welding electrode coatings. The novelty of the present work lies in the original methodology for fabricating a new electrode. An NFC was developed using pulsed radiation generated by functional ceramics based on lanthanum chromite. This work explored the thermal and mechanical stability of the nanostructured ceramics.

II. EXPERIMENTAL PART

In the current research, the A-815 activator was used as an activating component [18] in the coating charge of a rutile welding electrode, consisting of a mixture of powders with a granulometric composition of 2-10 microns, with a fraction of 5 microns containing at least 50%. The chemical composition of the A-815 activator is listed in Table I.

TABLE I. CHEMICAL COMPOSITION OF A-815 ACTIVATOR, WEIGHT %

Compound	FeO	SiO_2	Cr_2O_3	CaO	Al_2O_3	MgO	CuO
Amount (%)	32	26	17	15.3	4	3	1.5

The activating component A-815 was synthesized using the procedure presented in Figure 1 and consists of the following seven steps:

1. Preparation of the mixture of activator A-815.
2. Mixing in a planetary mill for 5 h.
3. Subsequent drying and annealing at a temperature of 800 °C for 2 h.
4. Grinding on a planetary mill for 5 h.
5. Annealing at 1000 °C for 2 h.
6. Annealing at 1200 °C for 2 h.
7. The resulting powder was placed for 15 min under radiators coated with functional ceramics based on lanthanum chromite, which generates pulsed radiation reaching 320 W/cm^2.

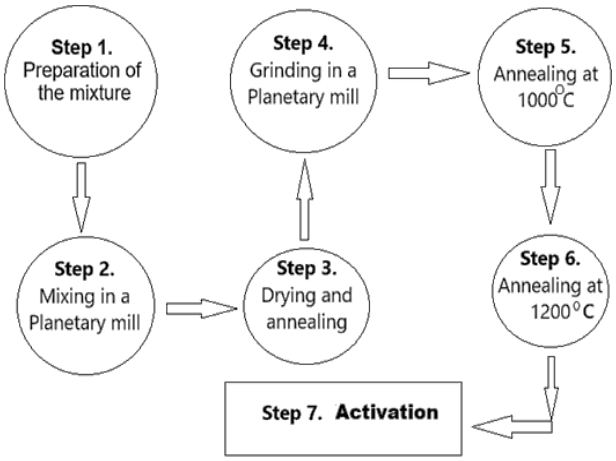

Fig. 1. Synthesis steps for the active component A-815.

The X-ray spectrum examination of the activated and non-activated samples, shown in Figure 2, revealed significant changes in the crystal structure and phase composition of the ceramics resulting from this process. Activation treatment decreased the metastable phase by accomplishing the main chemical processes.

The number of pulses for the inactive sample (Figure 2(a)) was up to 500 pulses, compared to 800 pulses for the active sample. The activation led to an increase in material crystallinity, as depicted in Figure 2(b), with minor fluctuations in the background line in clear distinction to the inactive sample. The chemical composition of the A-815 activator, particularly the high concentrations of FeO (32%) and Cr_2O_3 (17%), promotes the formation of stable complex spinel phases, such as chromite ($FeCr_2O_4$) and magnesiochromite ($MgCr_2O_4$), as illustrated in Figure 2(b).

The presence of MgO and Al_2O_3 further stabilized the spinel structures. Unlike the base material (Figure 2(a)), the patterns for the activated flux show high-intensity peaks corresponding to these spinels, which exhibit high melting points and superior thermal stability.

The addition of the activating component facilitates the transition of amorphous or metastable silicate-based phases (linked to the SiO_2-CaO system) into a more ordered crystalline matrix. In Figure 2(b), the "hump" characteristic of the amorphous phase is reduced, and new crystalline peaks emerge. This indicates that SiO_2 and CaO in the A-815 activator act as a fluxing matrix that hosts the reinforced spinel crystals.

The dominance of the spinel phase in the molten slag during welding is significant, as it maintains consistent viscosity and thermophysical properties over a wide temperature range. This stability prevents the erratic movement of the slag film and ensures a constant arc effect (driven by the SiO_2 and Cr_2O_3 components). Consequently, the phase stability achieved with A-815 resulted in a more concentrated heat input and a more uniform weld bead geometry than the processes without the activator.

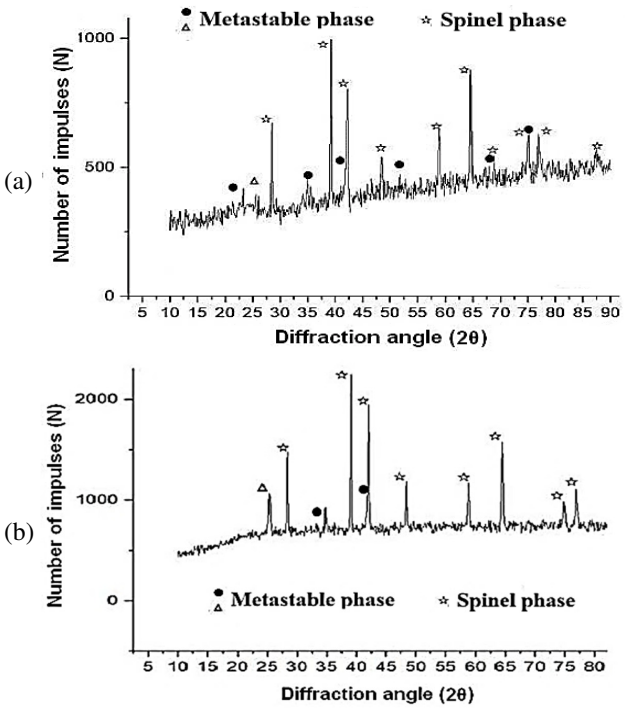

Fig. 2. X-ray diffraction spectra of the samples (a) before and (b) after activation.

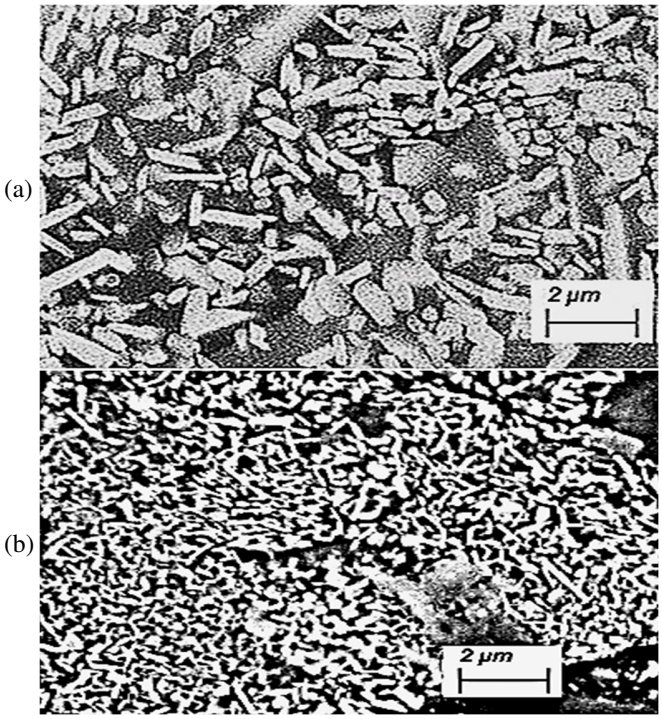

Fig. 3. Micrographs of the samples (a) before and (b) after activation.

Figure 3(a) presents a micrograph acquired by electronic microscopy of the sample before activation, which shows coarse crystallites. A significant decrease in the size of the crystallites and an increase in their density after activation are demonstrated in Figure 3(b). A substantial increase in the

proportion of interphase boundaries was found as a result of simple activation, initiating the generation of modulated IR radiation in the system under study. The high density of interfaces in Figure 3(b) is the physical trigger for the generation of modulated IR radiation.

The activating component of the A-815 brand prepared in this way was added to the coating charge of the welding electrode of the Rutile Type (RT). The chemical composition of the slag base was determined using the melting diagram of the TiO_2-SiO_2-CaO oxide system [19] in the following percentages: TiO_2 71.3%, SiO_2 17.7%, and CaO 11.0%, with a Basis Index (BI) of 0.206.

Table II presents the fabrication specifications of the electrodes under study. After applying the coating, the electrodes were dried at 80 °C for 40 min and then calcined at 180 °C for 60 min. The welding electrodes with different A-815 activator content are displayed in Table III.

TABLE II. SPECIFICATIONS OF WELDING ELECTRODES

Metal rod type and diameter	Sv08A wire, 4 mm in diameter
Activator A-815 proportions	From 0 to 16%.
Granulometric composition	Less than 315 μm
Liquid glass	Density 1.4 g/cm^3 and module 2.5
Ratio of a coating layer on the surface of the metal rod, thickness (D/d)	1.4-1.5

TABLE III. TESTED WELDING ELECTRODES

Composition of the coating of the welding electrode, weight%	**Appearance of welding electrodes**
100% RT (71.3% TiO_2 + 17.7% SiO_2 + 11.0% CaO)	
99% RT + 1% A-815	
98% RT + 2% A-815	
96% RT + 4% A-815	
92% RT + 8% A-815	
84% RT + 16% A-815	

The new electrodes were tested on a 4 mm thick plate made of St3sp steel using an inverter-type rectifier of the Jasic TIG-200P type. The welding arc was powered by direct current of reverse polarity at a welding current level of 140 A. The welding and technological properties of the welding electrodes listed in Table IV were determined using the method described in [20].

The welding and properties of welding electrodes include the stability of the burning of the arc of the welding electrode or the breaking length of the arc "L_{bla}", the diameter of the deposited point "ϕ_{dp}" or the quality of its formation, and the size of the visor at the end of the electrode "h_k".

To estimate the magnitude of these losses due to spattering, oxidation, and evaporation (fumes) during the burning of the arc, the so-called loss coefficient for waste and spatter "Ψ" was used, which is determined by:

$$\Psi = \frac{\alpha_p - \alpha_H}{\alpha_p} \times 100\% \quad (1)$$

In addition, the effect of the A-815 photocatalyst on the metal melting coefficient "α_p", deposition coefficient "$\alpha_н$", and loss factor for waste and splashing of electrode metal "Ψ", characterizing the process of welding and surfacing, was studied. The metal melting coefficient "α_p" shows how much electrode metal is melted per unit time per ampere of welding current, and is determined by:

$$\alpha_p = \frac{G_p}{I \cdot t} \quad (2)$$

where G_P (g) is the mass of the electrode metal melted during time t, I (A) is the welding current, t (h) is the arc burning time, and α_p (g/(A·h)) is the metal melting coefficient.

TABLE IV. WELDING AND TECHNOLOGICAL INDICATORS

Symbol of welding and technological indicators	**Definition**	**Aims and assessment method**
L_{bla}	The stability of the burning arc of the welding electrode	The breaking length of the arc, measuring the distance between the end of the electrode and the plate formed after surfacing
ϕ_{dp}	The quality of the welded joint formation	The diameter of the deposited point
h_k	The size of the visor at the end of the electrode, "method, and calcination modes on the tendency of welding electrodes "	The height of the peak at the end of the electrode
α_p	The metal melting coefficient	The electrode melting quantity coefficient
α_H	The surfacing coefficient	The surfacing coefficient
Ψ	The loss coefficient	Losses are due to spattering and oxidation.

The melting coefficient depends on the electrode material, the composition of its coating, type, polarity, and current density. During the welding process, the electrode heats up, which also affects the intensity of melting of the electrode metal. Before welding begins, the electrode is at room temperature; by the end of welding, it can heat up to 500 °C.

To evaluate the surfacing process, the surfacing coefficient "$\alpha_н$" is used, determined by:

$$\alpha_H = \frac{G_H}{I \cdot t} \quad (3)$$

where G_H (g) is the mass of the deposited electrode metal during time t, *and* α_H (g/(A·h)) is the metal melting coefficient.

The correct formation of the deposited point without external defects, such as undercuts, burns, cracks, and pores, indicates the high-quality formation of the welded joint. For values greater than 20% of the loss coefficient "Ψ", it is not advisable to use electrode welding. The influence degree of the A-815 additives in the electrode coating on the welding and technological properties of the welding electrodes was evaluated using the coefficient of determination R^2 [20]. The lowest possible value of R^2 is 0, and the highest possible value is 1. The coefficient of determination expresses how well the model predicts the results.

III. RESULTS AND DISCUSSION

Experiments were conducted to study the effect of the activating component on welding and technological properties. A-815 was introduced into the rutile-type electrode coating of the welding electrodes in quantities varying from 0 to 16%. The welding and technological properties are presented in Table V and Figures 4 and 5.

TABLE V. CRITERIA FOR SELECTING THE AMOUNT OF A-815 ACTIVATOR IN THE COMPOSITION OF THE RT COATING

#	Amount of A-185 in coating (%)	L_{bla} (mm)	ϕ_{dp} (mm)	h_k (mm)	a_p (g/A·h)	$\alpha_н$ (g/A·h)	Ψ (%)
1	0	13.4	12.3	1.8	6.81	6.12	10.2
2	1	13.3	11,8	1.4	6,37	5.76	9.60
3	2	14.8	11.5	1.2	6.44	5.87	8.90
4	4	13.2	11,0	2.1	6.90	6.06	12.1
5	8	13.0	12.6	1.6	7.21	6.47	10.1
6	16	12.9	11.4	1.8	7.95	7.18	9.60

The effect of the A-815 activator content in the coatings on the quality of weld formation showed that, in terms of the appearance of the deposited seams, the additives of the A-815 activator did not worsen the quality of weld formation, and in some cases, even improved it. Thus, when the activator content in the coating is up to 8%, the seam width expands with good seam formation. The improvement in weld formation can be attributed to the fact that the A-815 activator acts as a surfactant, facilitating the separation of droplets from the end of the electrode, which translates the metal transfer process during welding from coarse to fine [21], improving weld formation. The impact of the A-815 activator on welding quality and technological properties of the welding electrodes was investigated based on the properties listed in Table IV. The study results on the effect of coating composition on the welding and technological properties of welding electrodes are shown in Table V, and Figures 4 and 5. The results displayed in Table V represent the mean values derived from three independent measurements. The observed variability between the minimum and maximum values reflects the inherent stochastic nature of the arc-welding process. According to the statistical analysis presented in Table V and Figure 4, the low coefficients of determination for the h_k property (R^2 = 0.078) and weld seam formation (R^2 = 0.037) indicate that variations in the A-815 active component concentration, within the investigated range, do not exert a statistically significant linear influence on these parameters. The discontinuous arc length exhibits a poor linear fit (R^2 = 0.246), suggesting that while a slight trend may exist, it is largely obscured by measurement uncertainty and the complexity of plasma-chemical interactions. These low R^2 values support the conclusion that the studied properties remain stable regardless of the activator content, highlighting the robustness of the flux system. Adding up to 2% of A-815 to the coating enhances the breaking arc length "L_{bla}" of the electrode by more than 10%, as depicted in Table III and Figure 4. An additional increase in the activator diminishes the value of the breaking arc length.

The significantly improved breaking arc length "L_{bla}" observed with the addition of up to 2% activator A-815 to the electrode is due to the Impulse Tunneling Effect (ITE) [22]. ITE efficiency stems from its ability to focus the energy impulse, reducing the particle wavelength and enabling tunneling even at sub-barrier energies. Unlike conventional tunneling, ITE utilizes all incident radiation, creating a tightly focused energy band precisely tuned to the target process. This precise energy delivery maximizes melting efficiency.

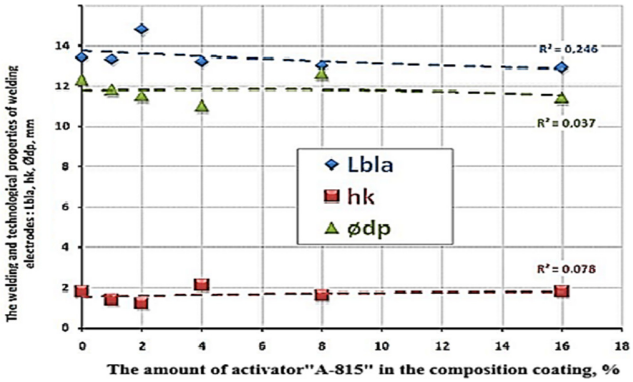

Fig. 4. Impact of the content of the activator A-815 in the electrode coating on L_{bla}, h_k, and ϕ_{dp} indicators.

This study revealed the effect of the A-815 activator on the size of the weld point diameter (ϕ_{dp}) and the quality of weld formation. It was found that the best results are observed with an activating component content of up to 8%. Simultaneously, the formation of the weld was improved (Table II) by increasing the width of the weld and the diameter of the deposited metal (Figure 4). It was also demonstrated that with the content of activator A-815 in the composition of the RT coating of 2%, there was a decrease in the size of the visor at the end of the electrode "h_k" by more than 33% (Figure 4). This had a positive effect on the stability of combustion and the re-ignition of the welding arc. The results of studying the dependence of the melting coefficient "α_p" on the content of the A-815 activator additive in the electrode coating, portrayed in Figure 5, showed an increase in "α_p" to 17% when the electrode was doped by up to 16% with A-815 activator. The significantly improved melting capacity observed with the addition of up to 2% activator A-815 to the electrode can be explained by the ITE [22].

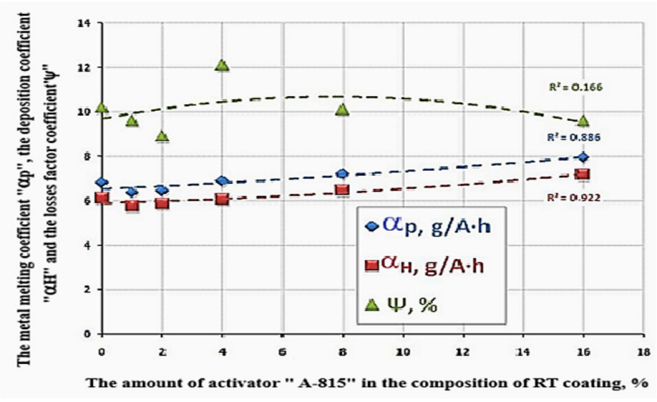

Fig. 5. Impact of the content of the activator A-815 in the electrode coating on α_p, α_H, and ψ indicators.

A similar effect of the A-815 activator was demonstrated when studying the dependence of the surfacing coefficient α_H on the content of this additive in the RT coating (Figure 5).

The experimental data exhibited a functional trade-off between process stability and deposition productivity. The maximum α_H was achieved at 16% A-815 content, showing a 17% increase compared to the standard RT coating. This enhancement in productivity at higher concentrations can be attributed to the intensified thermal concentration of the arc or exothermic reactions within the flux. However, peak arc stability is observed at significantly lower concentrations (~2%). This discrepancy suggests that while high activator content maximizes metal deposition rates, it may introduce minor arc fluctuations due to excessive vapor formation or changes in plasma conductivity.

From a practical point of view, the choice of A-815 concentration should be guided by the specific welding task. Adding 2% was proposed for precision welding, where arc control and seam quality were crucial, whereas a 16% concentration was optimal for high-volume surfacing operations, where maximizing the deposition rate was the primary objective. The effect of reducing waste and spatter losses to 12% was achieved by introducing the A-815 activator additive content of up to 4%. The activating component can generate pulse radiation during the heating of the coating during welding, which contributes to the effective removal of moisture. The residual moisture content of the coating decreases, resulting in improved welding and technological properties and improving the performance of the welding electrodes [21].

The findings of this study are limited to the specific experimental conditions investigated, including a single steel grade (St3sp), a fixed welding current of 140 A, and an electrode diameter of 4 mm. Although these results demonstrate the high potential of the A-815 activator, further research is proposed to evaluate its performance across a broader range of base materials and welding parameters, confirming the universal applicability of the proposed compositions.

IV. CONCLUSIONS

The present investigation examined the influence of incorporating the A-815 activator into the coating of a rutile welding electrode and explored its welding and technological properties. It was found that an increase in the breaking length of the electrode arc (L_{bla}) after spontaneous arc extinction by more than 10% was established when 2% of A-815 activator was added. Additionally, adding A-815 activator to the electrode coating composition up to 2% resulted in a 33% reduction in the value of the visor (h_k) at the end of the electrode. An increase of up to 17% was observed in both the melting (α_p) and surfacing (α_H) coefficients with an A-815 activator content of up to 16%. The coefficient of waste and spatter (Ψ) was reduced to 12% when the activator content reached up to 4%. From a practical perspective, using the active component A-815 as an additive in the coating composition of welding electrodes enhances their welding and technological properties by stabilizing arc burning and decreasing the size of the visor at the electrode's end. This improvement results in better weld formation quality and reduces the loss of molten electrode metal to waste and spatter, increasing labor productivity and decreasing the consumption of welding electrodes in the production of welded structures and products.

Future work will focus on comparing the new electrode with commercially available electrodes, such as E6013, in terms of weld morphology, microstructure, and mechanical properties.

REFERENCES

[1] J. H. Park, D. J. Min, and H. S. Song, "Amphoteric behavior of alumina in viscous flow and structure of CaO-SiO_2 (-MgO)-Al_2O_3 slags," *Metallurgical and Materials Transactions B*, vol. 35, no. 2, pp. 269–275, Apr. 2004, https://doi.org/10.1007/s11663-004-0028-2.

[2] C. Han *et al.*, "Viscosity Model for Iron Blast Furnace Slags in SiO_2–Al_2O_3–CaO–MgO System," *Steel Research International*, vol. 86, no. 6, pp. 678–685, 2015, https://doi.org/10.1002/srin.201400340.

[3] N. Siddiqi, B. Bhoi, R. K. Paramguru, V. Sahajwalla, and O. Ostrovski, "Slag–graphite wettability and reaction kinetics Part 1 Kinetics and mechanism of molten FeO reduction reaction," *Ironmaking & Steelmaking*, vol. 27, no. 5, pp. 367–372, Oct. 2000, https://doi.org/10.1179/030192300677679.

[4] Y. Liu, X. Lv, C. Bai, and B. Yu, "Surface Tension of the Molten Blast Furnace Slag Bearing TiO_2: Measurement and Evaluation," *ISIJ International*, vol. 54, no. 10, pp. 2154–2161, 2014, https://doi.org/10.2355/isijinternational.54.2154.

[5] D. Kalisz, "Influence of casting mold slag on the progress of casting process," *Archives of Metallurgy and Materials*, vol. 58, no. 1, pp. 35–41, 2013, https://doi.org/10.2478/v10172-012-0147-8.

[6] Y. Liu, H. Gu, Z. Leng, C. Peng, Z. Wang, and S. Zhang, "Study on the Optimization of Process Parameters for Submerged Arc Welding of Hydrogen Production Reactor Material," *Coatings*, vol. 14, no. 12, Dec. 2024, https://doi.org/10.3390/coatings14121548.

[7] R. Narayanan, K. Rameshkumar, A. Sumesh, B. Shankar, and D. T. Thekkuden, "Effect of Nano TiO2 Flux on Depth of Penetration and Mechanical Properties of TIG-Welded SA516 Grade 70 Steel Joints—An Experimental Investigation," *Metals*, vol. 15, no. 4, Apr. 2025, https://doi.org/10.3390/met15040399.

[8] J. Garg, S. B. Garg, and K. Singh, "Recycling of submerged arc welding slag into a hardfacing flux and its characterization," *Journal of Adhesion Science and Technology*, Jan. 2026, https://doi.org/10.1080/01694243.2026.2614361.

[9] C. S. Chai and T. W. Eacar, "Slag Metal Reactions in Binary CaF_2-Metal Oxide Welding Fluxes," *Welding Journal*, vol. 61, 1982.

[10] R. Kohno, N. Mori, K. Nagano, and T. Takami, "New fluxes of improved weld metal toughness for HSLA steels," *Welding Journal*, vol. 61, 1982.

[11] C. R. Heiple, J. R. Roper, R. T. Stagner, and R. J. Aden, "Surface-active element effects on the shape of GTA, laser, and electron-beam welds," *Welding Research Supplement*, pp. 72–77, Mar. 1983.

[12] A. G. Simonik, "The effect of contraction of the arc discharge upon the introduction of electro-negative elements," *Welding Production*, vol. 3, pp. 49–51, 1976.

[13] D. Klobčar, Tušek, M. Bizjak, S. Simončič, and V. Lešer, "Active flux tungsten inert gas welding of austenitic stainless steel AISI 304," *Metalurgija*, vol. 55, no. 4, pp. 617–620, Oct. 2016.

[14] S. V. Makarov and S. B. Sapozhkov, "Use of Complex Nanopowder (Al_2O_3, Si, Ni, Ti, W) in Production of Electrodes for Manual Arc Welding," *World Applied Sciences Journal*, vol. 22, pp. 87–90, 2013.

[15] S. Mahajan and R. Chhibber, "Design and Development of Shielded Metal Arc Welding (SMAW) Electrode Coatings Using a CaO-CaF_2-SiO_2 and CaO-SiO_2-Al_2O_3 Flux System," *JOM*, vol. 71, no. 7, pp. 2435–2444, July 2019, https://doi.org/10.1007/s11837-019-03494-9.

[16] T. Coetsee and F. J. De Bruin, "Thermochemical analysis of the behaviour of Cu in Ti nano-strand formation from low-temperature reaction of Al-Fe-Cu powder with CaF2-SiO2-Al2O3-MgO-MnO-TiO2 flux," *Chemical Thermodynamics and Thermal Analysis*, vol. 17, Mar. 2025, Art. no. 100160, https://doi.org/10.1016/j.ctta.2024.100160.

[17] R. Singh, "Welding and Joining Process," in *Applied Welding Engineering: Processes, Codes, and Standards*, 3rd ed., Oxford Cambridge, MA: Butterworth-Heinemann, 2020.

[18] R. Saidov, R. Rakhimov, K. Touileb, and S. Abduraimov, "A Study of the Influence of Additives of Nanostructured Functional Ceramics in the Coating of Welding Electrodes on their Welding and Technological Properties," *Engineering, Technology & Applied Science Research*, vol. 14, no. 6, pp. 18711–18717, Dec. 2024, https://doi.org/10.48084/etasr.8741.

[19] R. C. De Vries, R. Roy, and E. F. Osborn, "Phase Equilibria in the System CaO-TiO_2–SiO_2," *Journal of the American Ceramic Society*, vol. 38, no. 5, pp. 158–171, 1955, https://doi.org/10.1111/j.1151-2916.1955.tb14922.x.

[20] S. Chatterjee and J. S. Simonoff, *Handbook of Regression Analysis*, 1st ed. Wiley, 2012.

[21] D. P. Il'yaschenko, I. I. Chebotarev, and S. B. Sapozhkov, "Characteristics of droplet transfer of electrode metal during MMA depending on the chemical composition of the material of the rod of the coated electrode," *IOP Conference Series: Materials Science and Engineering*, vol. 939, Sept. 2020, Art. no. 012028, https://doi.org/10.1088/1757-899X/939/1/012028.

[22] R. K. Rakhimov, "Pulse Tunnel Effect: Fundamentals and Prospects for Application," *Computational nanotechnology*, vol. 11, no. 1, pp. 193–213, Apr. 2024, https://doi.org/10.33693/2313-223X-2024-11-1-193-213.